Hittite Journal of Science and Engineering, 2020, 7 (4) 297–311
ISSN NUMBER: 2148–4171
DOI: 10.17350/HJSE19030000199

Quantum Mechanical Calculation of Molybdenum and Tungsten Influence on the CrM-oxide Catalyst Acidity

Oyegoke Toyese[1] Fadimatu N. Dabai[1] Adamu Uzairur[2] and Baba El-Yakubu Jibril[1]
[1]Ahmadu Bello University, Department of Chemical Engineering, Zaria, Nigeria
[2]Ahmadu Bello University, Department of Chemistry, Zaria, Nigeria

ABSTRACT

Semi-empirical calculations were employed to understand the effects of introducing promoters such as molybdenum (Mo) and tungsten (W) on chromium (III) oxide catalyst for the dehydrogenation of propane into propylene. For this purpose, we investigated CrM-oxide (M = Cr, Mo, and W) catalysts. In this study, the Lewis acidity of the catalyst was examined using Lewis acidity parameters (Ac), including ammonia and pyridine adsorption energy. The results obtained from this study of overall acidity across all sites of the catalysts studied reveal Mo-modified catalyst as the one with the least acidity while the W-modified catalyst was found to have shown the highest acidity signifies that the introduction of Mo would reduce acidity while W accelerates it. The finding, therefore, confirms tungsten (W) to be more influential and would be more promising when compared to molybdenum (Mo) due to the better avenue that is offered by W for the promotion of electron exchange and its higher acidity(s). The suitability of some molecular descriptors for acidity prediction as a potential alternative to the current use of adsorption energies of the probes was also reported.

Article History:
Received: 2020/06/18
Accepted: 2020/11/02
Online: 2020/12/31

***Correspondence to**: Oyegoke Toyese, Ahmadu Bello University, Chemical Engineering, Zaria, NIGERIA*
E-Mail: oyegoketoyese@gmail.com
Phone: +234 703 047 91 06

Keywords:
Molecular descriptor; Metallic oxide; Semi-empirical calculation; Chromium oxide; Lewis acidity; Molecular probe.

INTRODUCTION

Propylene is one of the feedstocks in the petrochemical industries. It is commonly used as a precursor to producing important intermediates and products, such as isopropanol, polypropylene, propylene oxide, epichlorohydrin, and acrylonitrile [1, 2]. Several researchers have investigated the challenges encountered in propylene production which includes searching ways of increasing catalyst selectivity for propylene and decreasing catalyst deactivations. In addressing this challenge, a density functional theory (DFT) calculation was employed by Yan et al. [3] to propose a radical mechanism for propane dehydrogenation over Ga_2O_3 (100) where H abstraction by O(2) site was identified as a low energy barrier step. Ming et al. [4] employed DFT calculations to show that the introduction of tin into platinum catalyst lowers the energy barrier for propylene desorption and simultaneously increases the activation energy for propylene dehydrogenation, which has a positive effect on the selectivity of propylene production. Lauri et al. [5] also made related findings for the use of Pt-Sn catalyst, which lowered the coking rate while weakening the binding of propylene. Timothy [6] confirmed that PtGa alloy has superior catalytic properties than Sn-Ga alloy and similar properties to those deduced for Pt-Sn alloy as reported by Lauri et al. [5]. Stephanie et al. [7] found that an increase in hydrogen pressure lowers the coverage of deeply dehydrogenated coke precursors on the surface. Other similar findings have been reported in the literature [8, 9, 10, 11].

Recently, Oyegoke et al. [12] computationally showed that the chromium sites are highly acidic and reactive compared to the oxygen sites, identifying chromium sites as the leading active site in the promotion of propane dehydrogenation into propylene over Cr_2O_3 catalyst. Previous works such as Gascón et al. [13] have identified that the Cr_2O_3 catalyst in its pure form shows low catalyst selectivity for desired products and rapidly deactivates.

The search has shown that no work has investigated the role of foreign materials like molybdenum (Mo) and tungsten (W) in influencing the Lewis acidity of a catalyst site and how the material influences the performance of the Cr_2O_3 catalyst. Therefore, in this current

study, an approximation of the parameterized method 3 (PM3) of the semi-empirical theory was used to study the influence of foreign materials on the acidity of the chromium (III) oxide catalyst in a dehydrogenation process, using ammonia and pyridine (computationally) as molecular probes for the evaluation of the Lewis acidity of the sites. The suitability of some molecular descriptors as a potential substitute for using the probe's adsorption energies in the measurement of Lewis acidity (Ac) was evaluated. Its progress should reduce the time, cost, and efforts used in the evaluation of Ac.

THEORY

In molecular modeling, the molecular descriptors are diagrammatically presented in Fig. 1 establishing the relationship that exist among them. The electron affinity (EA) commonly defined as the capability of a ligand/catalyst/adsorbent to accept precisely one electron from a donor [14], which is known to be computed by chemists in the form:

$$EA \approx -ELUMO \tag{1}$$

The ionization energies (IE) known to be the energy required to remove electrons from the outermost shell is mathematically expressed in equation (2) in line with the report of Bendjeddou et al. [15].

$$IE \approx -EHOMO \tag{2}$$

The electronegativity (EN) of species can be mathematically expressed as:

$$EN, \chi = \frac{(\mathrm{IE} + \mathrm{EA})}{2} \approx -\left(\frac{ELUMO + EHOMO}{2}\right) \tag{3}$$

The chemical potential (CP) of species was defined to be the negative form of electron negativity (EN), and in line with the report of Bendjeddou et al. [15], it can be mathematically expressed as:

$$CP, \mu = -\frac{\partial E}{\partial N} \approx -\chi \tag{4}$$

Chemical hardness (CH) of the structure/site is a molecular descriptor that defines structural stability and reactivity. It is expressed in the form [14, 15]:

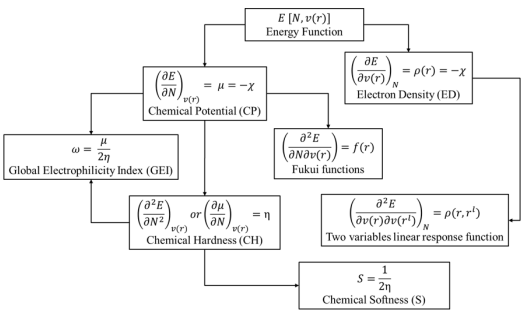

Figure 1. Molecular Descriptors employed in Molecular Modelling.

$$CH, \eta = \left(\frac{\partial^2 E}{\partial N^2}\right) = \left(\frac{\partial \mu}{\partial N}\right) \approx \left(\frac{IE - EA}{2}\right) \tag{5a}$$

$$CH, \eta \approx \left(\frac{ELUMO - EHOMO}{2}\right) \tag{5b}$$

Although, according to Luis et al. [16], some works tend to neglect the term ½, and when this is done, it approximates what is known as energy bandgap, E-gap.

Softness (S), known as the reciprocal of hardness often defined as the property of molecules that measure the degree of chemical reactivity of a given species [14, 16]. It usually is in the form:

$$S = \frac{1}{2\eta} \tag{6}$$

Global Electrophilicity Index (GEI) is a measure of the ability of a molecule to take up electrons [17, 18] and can be expressed in equation (5). It can also be said to be the tendency of an electrophile to acquire an extra amount of electron density, given by μ, and the resistance of a molecule to exchange electron density with the environment, given by Domingo et al. [19].

$$GEI, \omega \equiv \frac{\mu^2}{2\eta} \; or \; \frac{x^2}{2\eta} \tag{7}$$

Likewise, this parameter, ω is called the "electrophilicity index" and is considered to be a measure of electrophilic power, just as, in classical electrostatics, power is $\frac{v^2}{R}$, and μ and η serve the purpose of potential (V) and resistance (R), respectively [18, 19, 20].

COMPUTATIONAL BACKGROUND

In this study, the computations were carried out with the use of the Semi-empirical Parameterized Model 3 (PM3) calculation method in the Spartan 18 software package and ran on an HP 15 Pavilion Notebook (Intel Core i3 Processor @ 1.8 GHz and 6 GB RAM). This study involves the use of Spartan 18 in modeling and running all the molecular simulations while Microsoft Excel was used to aid both the mathematical and statistical analysis carried out. The molecular structures of the species involved in this study were sketched with the ACD/ChemSketch 11.

Choice of cluster structures

The molecular structures employed in representing chromium (III) oxide catalyst clusters or slabs were adopted from Compere et al. [21] and was found to be in line with the clusters reported in other studies [22, 23, 24, 25, 26, 27] while that of the probes and reactant was built to be in line with the molecular structure present in PubChem

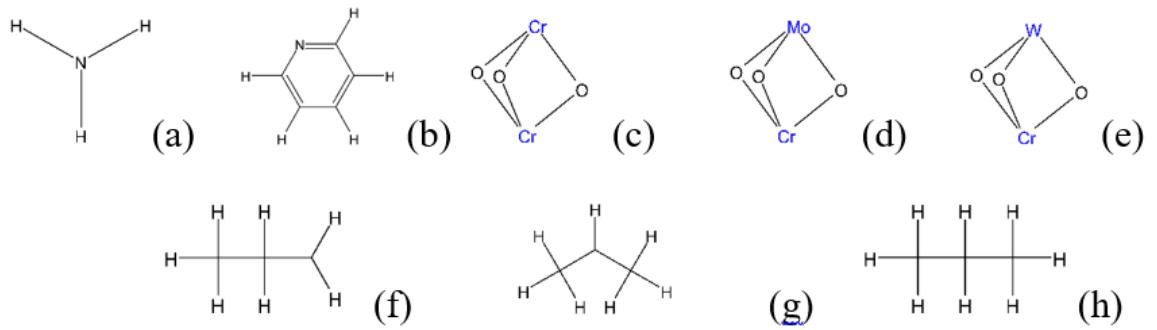

Figure 2. Molecular structure of molecular probes (a-b), unmodified catalyst cluster (c), modified catalyst cluster (d-e), Isopropyl species (f-g), propane (h).

online database. Besides, the modified surface of the catalyst (or modified form of the catalyst cluster) was built through the substitution of one chromium site on the chromium (III) oxide cluster with different metals such as molybdenum (Mo) and tungsten (W) to yield two modified catalyst clusters with names, Mo-modified, and W-modified, catalyst respectively. Fig. 2 pictorially displays the molecular structures employed in this study.

Ground-state geometrical optimizations

The catalyst, reactant, and molecular probe structures were built and minimized using the molecular mechanics (MMFF) method to remove strain energy to improve accuracy according to previous studies [28]. After this, the geometry optimizations and computations were carried out for the respective structures involved in this study using a PM3 method at the ground state. Infrared (IR) frequency, orbital, and energies calculations were carried out on all optimized structures, and the absence of any imaginary frequencies confirmed that each optimized structure was located at a minimum on its IR spectra plot. All computations are made with SCF tolerance of 10^{-9}. The PM3 basis set was employed because literature confirms it is one of the best for computations that involve transition metals, such as chromium [28, 29].

Molecular descriptors and adsorption energy computation

The heat of formation for the adsorbed species, catalyst slab, and catalyst slab with adsorbed species was calculated. The Infra-Red spectra, molecules' energies (E), and molecular parameters were evaluated from the computational approach employed, and the chemical hardness (CH), electronegativity (EN), chemical potential (CP), energy bandgap (E-gap), and global electrophilicity index (GEI) were calculated using Equation (1-7) [28]. Adsorption energies were calculated using the equation (6), which was in line with the literature [28, 30, 15, 31, 32]:

$$E_{ads} = E_{pq} - E_p - E_q \quad (8)$$

where E_{ads} is adsorption energy, E_p is the total energy of adsorbate (p), E_q is the total energy of free cluster or catalyst slab (q), and E_{pq} is the total energy of adsorbed cluster or catalyst slab with adsorbate (pq).

Lewis acidity evaluation

The Lewis acidity of different catalyst sites was evaluated using ammonia as a molecular probe. The sites' Lewis acidity was evaluated or rated using the adsorption energies calculated for the ammonia adsorption across the catalyst sites using the equation (8). The Lewis acidity of the catalyst sites was equally measured with the use of pyridine adsorption energies. This study approach was found to be in line with the method employed in the literature [33, 34, 12] in the measurement of Lewis acidity, which was taken to be a direct function of the probe adsorption energies across the sites. After this, the correlation that existed with the use of ammonia and pyridine was examined.

Acidity-reactivity correlation analysis

Molecular descriptors computed were correlated with Lewis acidity (Ac) of the catalyst, and their relationship with Ac of the catalyst site was evaluated using spearman's correlation analysis. The effects of different metals (or promoters) on the catalyst metallic sites' Lewis acidity were evaluated.

RESULTS AND DISCUSSION

Catalysts, Probe, Reactant, and Adsorption Species' Geometrical Optimization

The molecular properties computed from the geometry optimization of the probes, propane, and adsorption species are presented in Table 1 and Fig. 3 for the catalysts.

Table 1. Molecular Properties of the Probes, Catalysts, Isopropyl(s), and Propane.

Name	Formula	ELUMO (eV)	EHOMO (eV)	E (eV)	E Gap, (eV)	CH, η (eV)	EN, χ (eV)	CP, μ (eV)	GEI, ω (eV)
Ammonia	H_3N	3.33	-9.70	-0.13	13.03	6.51	3.18	-3.18	0.39
Pyridine	C_5H_5N	-0.01	-10.10	1.32	10.09	5.05	5.05	-5.05	1.26
Propyl-1	C_3H_7	3.22	-9.51	0.45	12.73	6.36	3.15	-3.15	0.39
Propyl-2	C_3H_7	3.22	-8.91	0.09	12.13	6.06	2.85	-2.85	0.33
Hydrogen	H_2	0.00	-13.07	2.26	13.07	6.54	6.54	-6.54	1.63
Propane	C_3H_8	3.71	-11.51	-1.02	15.22	7.61	3.90	-3.90	0.50

These results presented include the highest occupied molecular orbital energy (EHOMO), lowest unoccupied molecular orbital energy (ELUMO), ionization energy (IE), electron affinity (EA), chemical hardness (CH), electronegativity (EN), bandgap (E-Gap), and others. The energy bandgap (E-Gap) is known to be the absolute difference between the EHOMO and LUMO energies of any structure [15]. However, the optimized structures' geometry is presented in Table A6 in the Supplementary Information of this report.

Table 1 shows that propane has the most significant energy gap (15.22 eV), while pyridine has the shortest energy gap (10.09 eV), which implies that pyridine (molecular probe) would be the most reactive and least stable while propane will the least reactive and most stable materials. From the CrM-oxide surfaces, this study also identified that the unmodified surface of the chromium (III) oxide showed the shortest energy band gap (11.83 eV). In comparison, the surface-modified with molybdenum showed the most significant energy band gap (13.58 eV) in Fig. 3 (Table A1 in Supplementary Information). This result indicates that the presence of the molybdenum and tungsten increases the stability of the catalyst surface. In other words, it can be said that molybdenum and tungsten are harder molecules compared to unmodified Cr_2O_3 structures [15].

In the result of electronegativity (EN) presented in Fig. 3 (Table A1 in Supplementary Information), it was observed that chromium (III) oxide has the highest electron affinity (8.60 eV) while isopropyl showed the least electronegativity (2.85-3.15 eV). These findings imply that the chromium (III) oxide has a high ability to accept electrons, while isopropyl shows the least potential for electron reception. It further shows that the presence of tungsten and molybdenum decreases the EN of Cr_2O_3 catalyst, which agreed with David [35] showing that tungsten (W) and molybdenum (Mo) displayed a relative lower EN compared to chromium (Cr).

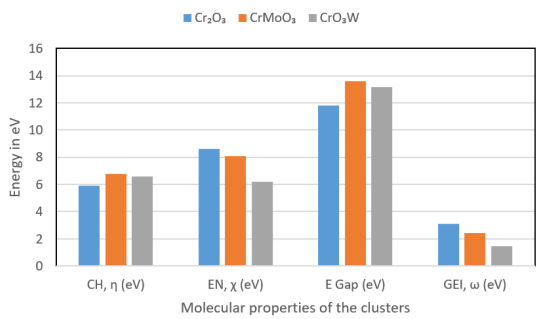

Figure 3. Molecular Properties of the Catalysts (Note: E Gap = Band Gap, CH = Chemical Hardness, EN = Electronegativity, GEI = Global Electrophilicity Index).

Similarly, it was observed that unmodified chromium (III) oxide has the highest LUMO energy (-2.68 eV), while propane has the lowest LUMO energy (3.71 eV). These findings imply that unmodified chromium (III) oxide possesses a high ability to attract electrons to its surface while propane possesses the least electron attraction ability. This result shows that the unmodified chromium (III) oxide is most likely to accept electrons from the adsorbates like propane and propylene during the binding process. It is evident from its results obtained as 3.12 eV for the global Electrophilicity Index (GEI), which shows that unmodified chromium (III) oxide is highly reactive and good electrophile due to its high GEI value [18].

The chemical hardness (CH) results in Table 1, and Fig. 3 shows that pyridine has the lowest IE (5.05 eV), while propane has the highest chemical hardness (7.61 eV), indicating that propane has the highest resistance towards the deformation of its electron cloud of atoms. It further shows that the presence of tungsten and molybdenum increases the chemical hardness of Cr_2O_3 catalyst (as shown in Fig. 3), which agreed with the literature [35] showing that tungsten (W) and molybdenum (Mo) displayed a relatively higher chemical hardness compared to chromium (Cr). Similarly, it was observed that isopropyl species has the highest HOMO energy (-9.51 eV to -8.91 eV) while molybdenum modified chromium (III) oxide surface has the lowest HOMO energy (-14.89 eV). This finding indicates that pyridine would quickly release electrons compared to other species and surfaces modified with metals like tungsten and molybdenum, which will not quickly release electrons for a reaction process [36].

Table 2. Lewis acidity of Cr_2O_3 using Ammonia probe.

Site	ELUMO (eV)	EHOMO (eV)	E (eV)	Ac_Cr_2O_3	CH, η (eV)	EN, χ (eV)	CP, μ (eV)	GEI, ω (eV)
Cr	4.56	-4.33	-8.01	-7.00	4.45	-0.11	0.11	0.00
O	8.70	0.66	-4.17	-3.16	3.41	-4.68	4.68	1.45

Table 3. Lewis acidity of $CrMoO_3$ using Ammonia probe.

Site	ELUMO (eV)	EHOMO (eV)	E (eV)	Ac_$CrMoO_3$	CH, η (eV)	EN, χ (eV)	CP, μ (eV)	GEI, ω (eV)
Cr	3.98	-5.89	-2.31	-1.45	4.94	0.96	-0.96	0.05
Mo	4.54	-6.88	-7.99	-7.13	5.71	1.17	-1.17	0.06
O	10.41	-0.50	-5.44	-4.58	5.46	-4.96	4.96	1.02

Table 3. Lewis acidity of $CrWO_3$ using Ammonia probe.

Site	ELUMO (eV)	EHOMO (eV)	E (eV)	Ac_$CrWO_3$	CH, η (eV)	EN, χ (eV)	CP, μ (eV)	GEI, ω (eV)
Cr	4.96	-5.03	-14.26	-11.87	5.00	0.04	-0.04	0.00
W	4.28	-2.10	-11.48	-9.09	3.19	-1.09	1.09	0.09
O	9.50	-0.30	-5.82	-6.02	4.65	-4.60	4.60	1.01

Lewis Acidity Evaluation of CrM-Oxide Catalyst Site

Here, the different potential sites on both unmodified and modified chromium (III) oxide surfaces were evaluated for acidity using the adsorption energies (Eads). This study evaluated the use of pyridine, and ammonia adsorption energy was employed. In contrast, the use of other molecular descriptors such as LUMO energy, electronegativity (EN), chemical hardness (CH), and global Electrophilicity index (GEI) as potential Lewis acidity descriptors were evaluated. The method employed in the Lewis acidity computation is in line with that employed in past works [33, 37, 12].

Adsorption of Ammonia on CrM-Oxide Surface

The ammonia adsorption energies tagged 'Ac_Cr_2O_3, Ac_$CrMoO_3$, and Ac_$CrWO_3$' for the respective sites are presented in Table 2-4. The evaluation of the result identifies that the chromium (Cr) site on the unmodified chromium (III) oxide showed the highest Lewis acidity while the oxygen (O) site was found to be the lowest Lewis acidity. The findings agreed with the literature [38, 39], which identified Cr as the most active site.

This deduction indicates that oxygen (O) is the most basic Lewis site, while chromium (Cr) is the most acidic Lewis site on unmodified chromium (III) oxide surface. According to Michorczyk et al. [40, 39], this implies that Cr, which is unsaturated, would be more unstable and be more active for adsorption of propane, unlike the oxygen sites, which agree with the finding of Gascón et al. [13] that confirms the Cr site to be active.

CrM-oxide surface with chromium site is substituted with molybdenum; the finding from the results presented in Table 3 shows that the Lewis acidity trend of the sites on the surface is molybdenum (Mo) > oxygen (O) > chromium (Cr). This finding indicates that the chromium (Cr) site would be the most basic Lewis site, while molybdenum (Mo) would be the most acidic Lewis site.

Further study of Table 4 shows that the chromium (Cr) site is the most acidic Lewis site while oxygen (O) shows the least acidic Lewis site on the surface modified with substitution of chromium with tungsten (W). It implies that the oxygen (O) site is the most basic Lewis site.

The overall assessment of the different catalyst Lewis acidity shows that $CrWO_3$ (-11.87 eV) > $CrMoO_3$ (-7.13 eV) > Cr_2O_3 (-7.00 eV) in their increasing order of acidity. This deduction finds an agreement with the reports of Bailey et al. [41] and Chen et al. [42], which indicates that tungsten is more promising when compared to Mo-modified Cr_2O_3 due to the high Lewis acidity of W-modified Cr_2O_3.

Adsorption of Pyridine on CrM-Oxide Surfaces

Here, this study's findings on the evaluation of Lewis acidity of the catalyst sites using pyridine as the molecular probe are presented in Table 5.

Table 5. Lewis acidity of Cr_2O_3 using Pyridine probe.

Site	ELUMO (eV)	EHOMO (eV)	E (eV)	Ac_Cr_2O_3	CH, η (eV)	EN, χ (eV)	CP, μ (eV)	GEI, ω (eV)
Cr	1.94	-5.54	-6.62	-7.06	3.74	1.80	-1.80	0.22
O	8.28	1.38	-3.68	-4.12	3.45	-4.83	4.83	1.69

Table 6. Lewis acidity of $CrMoO_3$ using Pyridine probe.

Site	ELUMO (eV)	EHOMO (eV)	E (eV)	Ac_$CrMoO_3$	CH, η (eV)	EN, χ (eV)	CP, μ (eV)	GEI, ω (eV)
Cr	4.46	-2.25	-2.66	-3.25	3.35	-1.11	1.11	0.09
Mo	2.08	-6.83	-6.64	-7.23	4.46	2.38	-2.38	0.32
O	5.05	-0.86	-3.76	-4.35	2.95	-2.09	2.09	0.37

Table 7. Lewis acidity of $CrWO_3$ using Pyridine probe.

Site	ELUMO (eV)	EHOMO (eV)	E (eV)	Ac_$CrWO_3$	CH, η (eV)	EN, χ (eV)	CP, μ (eV)	GEI, ω (eV)
Cr	2.05	-5.32	-12.23	-11.29	3.69	1.63	-1.63	0.18
W	3.14	-3.97	-10.72	-9.78	3.55	0.42	-0.42	0.01
O	5.34	-1.14	-10.02	-9.08	3.24	-2.10	2.10	0.34

A trend similar to the one deduced from the use of ammonia as the probe was observed showing that the chromium (Cr) site on the unmodified chromium (III) oxide showed its high Lewis acidity (pyridine adsorption energy) while the oxygen (O) site was found to be the lowest Lewis acidity. This result indicates that oxygen (O) is the most basic Lewis site, while chromium (Cr) is the most acidic Lewis site on unmodified chromium (III) oxide surface. This deduction implies that pyridine adsorption energy studies confirm the Cr site as the most acidic and active site, in agreement with Michorczyk et al. [40] report.

The finding on the CrM-oxide surface with chromium site is substituted with molybdenum presented in Table 6 shows that the chromium (Cr) site would be the most basic Lewis site. In contrast, molybdenum (Mo) would be the most acidic Lewis site when the pyridine probe is employed, which was found to agree with the initial deductions made for the use of ammonia as the molecular probe.

Table 7 showed that the chromium (Cr) site is the most acidic Lewis site, while oxygen (O) shows the least acidic Lewis site on the surface modified with substitution of chromium with tungsten (W). It indicates that the oxygen (O) site is the most basic Lewis site. These findings agree with the deductions made from the use of ammonia as molecular probes.

The trend of the catalyst Lewis acidity observed for $CrWO_3$, $CrMoO_3$, and Cr_2O_3 was found to show a similar order with that obtained when ammonia was used as pyridine. Likewise, the deductions agree with the literature [41, 42], which indicates that tungsten would perform better than Mo-modified Cr_2O_3 due to the high Lewis acidity of W-modified Cr_2O_3 surface.

Correlation of Catalyst Lewis Acidity & Molecular Descriptors

This analysis tends to evaluate the correlation of Lewis acidity measured in terms of ammonia and pyridine adsorption energy presented in Table A2-A4 of the Supplementary Information, including results showing the ammonia and pyridine probe Lewis acidity relationship with other molecular descriptors such as ELUMO, EHOMO, CH, EN, CP, and GEI as potential Lewis acidity descriptors using the results presented in Table 2 – 7.

The correlation analysis results for the chromium site shows a correlation coefficient of +1.00 for the relation between ammonia and pyridine Lewis acidity of chromium site, r (aAc_Cr / pAc_Cr) evaluated in Table A2 of the Supplementary Information. The findings obtained from the analysis reveals that there exists a good and direct relationship in the use of ammonia or pyridine as a molecular probe for the assessment of Lewis acidity, which was found to agree with the literature [32, 12], which made the similar deduction that shows a unity of result output in the use of ammonia and pyridine in the measurement of Lewis acidity. The results equally show that there is a good relationship for GEI (-0.95), CP (-0.99), EN (-0.99), E (+1.00), EHOMO (-0.90), and ELUMO (-0.89) except for CH (-0.53) that shows the

fair correlation for the deductions made from the used ammonia and pyridine for the chromium site evaluation.

Furthermore, it was identified that a good relationship thus exists for all the molecular descriptors aforementioned except for aCH (-0.02) with Lewis acidity deduced via the use of ammonia as a molecular probe. Nevertheless, when pyridine was employed, all molecular descriptors showed a good correlation or relationship with the Lewis acidity as well except for the ammonia HOMO energy (-0.49) and aCH (-0.12) that shows a weak correlation as r is -0.4 (as shown in Table A2). Findings from the study of results presented in Table A2 of the Supplementary Information identifies GEI, CP, EN, and ELUMO descriptors as better potential substitutes for the use of probe adsorption energies for the study of Lewis acidity.

In the study of substituted metal or introduced metal sites, the correlation analysis result presented in Table A3 of the Supplementary Information shows a correlation coefficient of +1.00 for the relationship between ammonia and pyridine Lewis acidity of chromium site, r (aAc_M / pAc_M). The results imply that the Lewis acidity evaluation with the use of ammonia positively agrees well with that deduced with the use of pyridine. These findings are similar to the reports of Liu et al. [34] and Oyegoke et al. [12], which made a similar deduction that shows a unity of result outputs in using ammonia and pyridine for the measurement of Lewis acidity. Moreover, analogous correlations were also obtained for all other descriptors except for GEI (-0.51) and ELUMO (-1.00), which shows a negative correlation (where GEI correlation was found below).

Also, all molecular descriptors were found to agree with Lewis acidity evaluated via the use of ammonia except for pyridine ionization energy, i.e., pCH (+0.54). However, when pyridine is used as a molecular probe, only ammonia aCH was found to show a fair relationship with the Lewis acidity with a correlation coefficient of r = +0.62, unlike others that showed a better correlation. The findings indicate that chemical hardness (CH) would be a weak substitute for molecular probe adsorption energy as a molecular descriptor to measure Lewis acidity.

The correlation assessment results for Lewis acidity presented in Table A4 of the Supplementary Information indicate that the r (aAc_O / pAc_O) is +0.90, which signifies that there is a good and positive agreement between the use of ammonia and pyridine as a molecular probe in the evaluation of oxygen site Lewis acidity. Moreover, the ELUMO (-0.89), EHOMO (+0.96), CH (-0.98), and GEI (+1.00) showed a good correlation, while CP (-0.32) and EN (-0.32) showed a weak correlation for the outcomes obtained from the use of ammonia and pyridine comparison. Further study of the parameters shows that all molecular descriptors show a good relationship with the Lewis acidity measured with the use of ammonia except for aEN (-0.20), aCP (+0.20), aELUMO (-0.46), and pCH (+0.42), which indicates a weak correlation with the Lewis acidity. ELUMOs (p = +0.47, a = 0.00), aHOMO (+0.39), and aCH (-0.16) showed a weak correlation when pyridine was employed to evaluate the Lewis acidity of the oxygen sites. The findings imply that the use of ELUMOs, aHOMO, CHs, aEN, and aCP as potential molecular descriptors would result in a poor prediction for oxygen sites.

A positive and good correlation was identified for aEN, aGEI, and pELUMO, while aELUMO, pEN, and pGEI showed a negative and good correlation from the results (Table A2 in Supplementary Information) for Cr-Site. In the correlation analysis of M-site presented in Table A3 of the Supplementary Information, aGEI and pELUMO was found to show a good and positive correlation with Lewis acidity. In contrast, aELUMO was found to be the only good and negative correlation for Lewis acidity across M-site. A good and positive correlation was found for aELUMO and pEN, while a negative correlation was found for GEIs and pELUMO with Lewis acidity at O-site.

The correlation analysis of all the molecular descriptors reveals GEIs, pCP, pEN, and pEHOMO correlate well with the Lewis acidity evaluated at all the sites using ammonia, pyridine, and ammonia, respectively. This finding confirms the pyridine-based descriptors such as GEI, CP, EN, and EHOMO as proper molecular acidity descriptors. At the same time, GEI was the only ammonia-based descriptor that could only serve as an alternative or substitute for molecular probe adsorption energy to measure catalyst site Lewis acidity.

The nature of the relationship between catalyst surfaces molecular descriptors such as ELUMO, EHOMO, E Gap, CH, EN, CP, and GEI in Fig. 4 (Table A1 of the Supplementary Information) and Lewis acidity of the catalyst sites (such as Cr, M, and O in Table 2-7) are presented in Table A5 of the Supplementary Information. Findings from this study shows that the correlation coefficient average of the

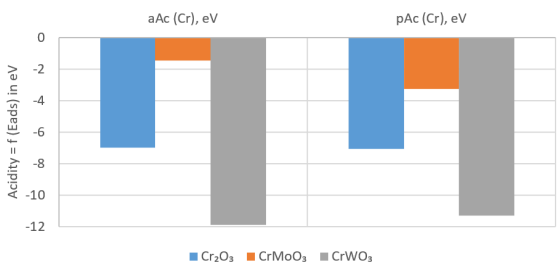

Figure 4. Result of Chromium (Cr) Site Acidity on the CrM-Oxide Catalyst Surface.

molecular descriptors goes in the trend of CH (-0.23) < E Gap (-0.23) < ELUMO (-0.81) < GEI (+0.82) < CP (-0.90) < EN (+0.90) < EHOMO (-0.92). This result indicates that EN and E Gap correlate poorly while other catalyst surface descriptors such as ELUMO, GEI, CP, EN, and EHOMO correlate well, but only EHOMO correlates best with the Lewis acidity of different catalyst sites. Therefore, this study identifies that GEI, ELUMO, EHOMO, CP, and EN would suitably describe the intensity of catalyst surface Lewis acidity without the use of molecular probe adsorption energy. However, EHOMO describes it best as it is displayed in Table A5 of the Supplementary Information. This finding was contrary to Jupp et al. [43], which present that GEI would be the best Lewis acidity descriptor.

Assessment of Introduced Metals (M) Effect on CrM-oxide Catalyst Acidity

Effect of introducing metal (M) on the Cr-site Lewis acidity on the CrM-oxide

Here, the chromium site on a surface modified with tungsten was the most acidic with -11.29 to -11.87 eV adsorption energy, while the molybdenum modified surface showed a lower acidic site with adsorption energy -1.45 to -3.63 eV as shown in Fig. 4.

The order of the chromium site acidity was in the following order: $CrWO_3 > Cr_2O_3 > CrMoO_3$. This finding reveals that molybdenum on the chromium (III) oxide surface reduces the chromium site acidity while tungsten increases.

Effect of introduced metal (M) on the M-site Lewis acidity on the CrM-oxide surface

Fig. 5 shows that for the different metal sites (molybdenum and tungsten), the molybdenum modified surface showed a higher acidity (with adsorption energy of -7.13 to -7.23 eV) compared to the unmodified Cr_2O_3 surface. In comparison, the tungsten modified surface was found to be the most acidity site (with adsorption energy of -9.09 to -9.78 eV). The order of the introduced or different metal site Lewis acidity was identified to be in the trend of $CrWO_3 > CrMoO_3 > Cr_2O_3$.

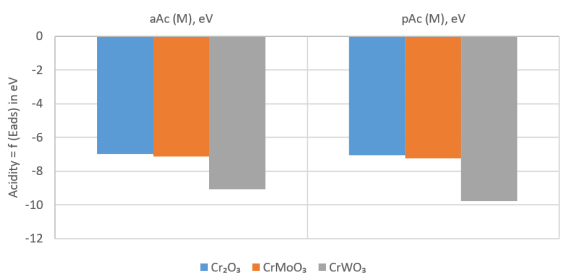

Figure 5. Result of Foreign Metal (M) Site Acidity on the CrM-Oxide Catalyst Surface.

This study shows that both molybdenum and tungsten metal sites exhibit a higher Lewis acidity than their respective chromium sites, signifying that the metals' presence increases the Lewis acidity of the catalyst surface for better exchange of electrons.

Effect of introduced metal (M) on the O-site Lewis acidity on the CrM-oxide surface

In the evaluation of the Lewis acidity across the oxygen sites on different catalyst clusters, CrM-oxide (where M = Cr, Mo, and W metals), the results collected presented in Fig. 6 shows that oxygen sites found on surface modified with tungsten exhibits the highest Lewis acidity with an adsorption energy of -6.060 to -9.08 eV while the oxygen sites on the unmodified surface exhibit the least Lewis acidity with an adsorption energy of -3.16 to -4.12 eV.

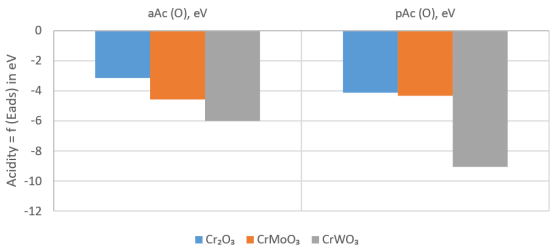

Figure 6. Result of Oxygen (O) Site Acidity on the CrM-Oxide Catalyst Surface.

However, the oxygen sites' Lewis acidity was in the trend: $CrWO_3 > CrMoO_3 > Cr_2O_3$. This trend order shows that the presence of Mo and W in the modified catalyst surface results in an increase in the Lewis Acidity of oxygen site on the catalyst's respective surfaces.

CONCLUSION

With the use of the parameterized method 3 (PM3) of the semi-empirical theory, this work was able to investigate the influence of molybdenum (Mo) and tungsten (W) on the acidity of the chromium (III) oxide catalyst, using ammonia and pyridine (computationally) as molecular probes for the assessment of the catalyst sites' Lewis acidity. The suitability of some molecular descriptors for Lewis acidity prediction was also investigated as a potential alternative to the current use of probes' adsorption energies.

This study's findings indicate that introducing the Mo and W on chromium (III) oxide catalyst increases its stability due to the broad energy bandgap identified for the foreign metals' presence. Likewise, the presence of the foreign metals (Mo and W) was found to have increased the Cr_2O_3

catalyst chemical hardness (CH) while, on the other side, resulting in a decrease in electronegativity (EN) of Cr_2O_3 catalyst, which would aid in preventing the production of undesired products and cokes when used in dehydrogenation process. Among the adsorbates considered in this study, pyridine (molecular probe) was found to be the most reactive and least stable, while propane was found to be the least reactive and most stable materials.

The evaluation of the catalyst Lewis acidity with the use of ammonia (as the molecular probe) reveals that chromium (Cr) is the most acidic site across on the catalyst surfaces when compared to its oxygen (O) site. Although introducing foreign metals like Mo and W on it indicates that the catalyst surfaces modified with molybdenum (Mo) would suppress the catalyst's acidity. At the same time, tungsten (W) would accelerate the acidity, indicating that the introduction of Mo reduces the acidity while W increases it. The study further identifies that these findings were in line with that made from the use of pyridine.

Moreover, the chromium site acidity order reveals that the presence of molybdenum on the Cr_2O_3 surface reduces the chromium site acidity while tungsten increases it, unlike the oxygen acidity that increases in the presence of either Mo or W. The acidity of introduced (or foreign) metal sites was identified to be more acidic relative to unmodified Cr_2O_3, which increases the total catalyst acidity for better exchange of electrons due to their higher Lewis acidity(s) when compared to their respective chromium sites on their modified surfaces. This finding shows that tungsten would be more promising when compared to Mo-modified Cr_2O_3 due to the high Lewis acidity of W-modified Cr_2O_3 for the dehydrogenation process.

ACKNOWLEDGMENT

The authors wish to thank the management of the Chemical Engineering Department of ABU Zaria for their constant interest and valuable advice in this project. Also, the first author wishes to acknowledge the financial support of the PTDF that made my program a success.

ABBREVIATION

aAc	Ammonia-based Lewis acidity of …
pAc	Pyridine-based Lewis acidity of …
CP	Chemical potential, μ
CH	Chemical hardness, η
Cr	Chromium Site
DFT	Density functional theory
E	Total energies of the structures
EA	Electron affinity
Eads	Adsorption energy
E-gap	Bandgap
EHOMO	The energy of HOMO orbital
ELUMO	The energy of LUMO orbital
EN	Electronegativity, χ
Ep	The total energy of adsorbate (p)
Epq	The total energy of the catalyst slab with adsorbate (pq)
Eq	The total energy of the free cluster or catalyst slab (q) or E-surface
H	Hydrogen atom
HOMO	Highest occupied molecular orbital
IE	Ionization energy
GEI	Global electrophilicity index, ω
IR	Infrared spectra
L	The bond length in angstrom
LUMO	Lowest unoccupied molecular orbital
M	Foreign metal introduced metal or promoter sites
MMFF	Molecular mechanics force field
Mo	Molybdenum atom
P1	Propyl-1
P2	Propyl-2
PM3	Parameterized method three approximation of semi-empirical theory
r	Correlation coefficient

r (aAc) The correlation coefficient of ammonia-based Lewis acidity (aAC) to …

r (pAc) The correlation coefficient of pyridine-based Lewis acidity (pAC) to …

W Tungsten atom

References

1. Budavari S. Propylene. The Merck Index, 12th ed., New Jersey: Merck & Co., 1996, p. 1348–1349.
2. Ren Y, Zhang F, Hua W, Yue Y, Gao Z. "ZnO supported on high silica HZSM-5 as new catalysts for dehydrogenation of propane to propene in the presence of CO2," Catalysis Today, 2009; 148(3-4): 316-322.
3. Yan L, Zhen H, Jing L, Kang-Nian F. "Periodic Density Functional Theory Study of Propane Dehydrogenation over Perfect Ga2O3 (100)," Surface, J. Phys. Chem. C, 2008, 112(51):20382–20392.
4. Ming L, Yi A, Xing G, Zhi J, De C. "First-Principles Calculations of Propane Dehydrogenation over PtSn Catalysts," ACS Catalysis, 2012, 2(6):1247–1258.
5. Lauri N, Karoliina H. "Selectivity in Propene Dehydrogenation on Pt and Pt3Sn Surfaces from First Principles," ACS Catalysis, 2013, 3(1):3026–3030.
6. Timothy H. "Computational study of the catalytic dehydrogenation of propane on Pt and Pt3Ga catalysts," Doctoral Thesis, 2015.
7. Stephanie S, Maarten K, Vladimir V, Evgeniy A, Marie-Françoise R, Guy B. "The Positive Role of Hydrogen on the Dehydrogenation of Propane on Pt (111)," ACS Catalysis, 2017, 7(11): 7495–7508.
8. Biloen P, Dautzenberg F, Sachtler W. "Catalytic dehydrogenation of propane to propene over platinum and platinum-gold alloys," Journal of Catalysis, 1977, 50(1): 77-86.
9. Benco L, Bucko T, Hafner J. "Dehydrogenation of propane over ZnMOR. Static and dynamic reaction energy diagram," Journal of catalysis, 2011, 277(1): 104-116.
10. Li H, Yue Y, Miao C, Xie Z, Hua W, Gao Z. "Dehydrogenation of ethylbenzene and propane over Ga2O3–ZrO2 catalysts in the presence of CO2," Catalysis Communications, 2007, 8(9): 1317-1322.
11. Ming-Lei Y, Yi-An Z, Chen F, Zhi-Jun S, De C, Xing-Gui Z. "DFT study of propane dehydrogenation on Pt catalyst: effects of step sites," Physical Chemistry, Chemical Physics, 2011, 13(1): 3257–3267.
12. Oyegoke T, Dabai FN, Uzairu A, Jibril BY. "Insight from the Study of Acidity and Reactivity of Cr2O3 Catalyst in Propane Dehydrogenation: A Computational Approach," Bayero Journal of Pure and Applied Sciences, 2018, 11(1): 178-184.
13. Gascón J, Téllez C, Herguido J, Menéndez M. "Propane dehydrogenation over a Cr2O3/Al2O3 catalyst: transient kinetic modeling of propene and coke formation," Applied Catalysis A: General, 2003, 248(1-2): 105-116.
14. Parthasarathi R, Subramanian V, Royb D, Chattaraj P. "Electrophilicity index as a possible descriptor of biological activity," Bioorganic & Medicinal Chemistry, 2004, 12(1): 5533-5543.
15. Bendjeddou A, Abbas T, Gouasmia AK, Villemin D. "Molecular structure, HOMO-LUMO, MEP, and Fukui function analysis of some TTF donor substituted molecules using DFT (B3LYP) calculations," Int Res J Pure Appl Chem, 2016, 12(1):1-9.
16. Parr R, Szentpály L, Liu S. "Electrophilicity Index," J. Am. Chem. Soc., 1999, 121(1): 1922-1924.
17. Pratim K, Utpal S, Debesh R, "Electrophilicity Index," Chemical Review, 2006, 106(1): 2065-2091.
18. Domingo L, Ríos-Gutiérrez M, Pérez P. "Applications of the Conceptual Density Functional Theory Indices to Organic Chemistry Reactivity," Molecules, 2016, 21(748): 1-22.
19. Robert G, La´szlo V, Shubin L. "Electrophilicity Index," J. Am. Chem. Soc., 1999, 121(1): 1922-1924.
20. Compere C, Costa D, Jolly LH, Maugerc E, Giessner–Prettre C. "Modeling of the adsorption on Cr2O3 clusters of small molecules and ions present in seawater. A preliminary non-empirical study," New J. of Chem, 2000, 24(12): 993-998.
21. Yanbiao W, Xinxin G, Jinla W. "Comparative DFT Study of Structure and Magnetism of TMnOm (TM = Sc - Mn, n = 1 - 2, m = 1 - 6) Clusters," Physical Chemistry Chemical Physics, 2010, 12 (1): 2471-2477.
22. Veliah S, Xiang K, Pandey R, Recio J, Newsam J. "Density Functional Study of Chromium Oxide Clusters: Structures, Bonding, Vibrations, and Stability," J. Phys. Chem. B, 1997, 102(1): 1126-1135.
23. Garrain PA, Costa D, Marcus P. "Biomaterial– biomolecule interaction: DFT-D study of glycine adsorption on Cr2O3.," The Journal of Physical Chemistry C, 2010, 115(3): 719-727.
24. Shah EV, Roy DR. "Magnetic switching in Crx (x= 2–8) and its oxide cluster series," Journal of Magnetism and Magnetic Materials, 2018, 451: 32-37.
25. Dzade N, Roldan A, de Leeuw N. "A density functional theory study of the adsorption of benzene on hematite (α-Fe2O3) surfaces," Minerals, 2014, 4(1): 89-115.
26. Lau KC, Kandalam AK, Costales A, Pandey R. "Equilibrium geometry and electron detachment energies of anionic Cr2O4, Cr2O5, and Cr2O6 clusters," Chemical physics letters, 2004, 393 (1-3): 112-117.
27. Warren J. A Guide to Molecular Mechanics and Quantum Chemical Calculations, Irvine, CA: Wavefunction, 2003.
28. Warren H, Sean O. Spartan 16 for Windows, Macintosh and Linux: User Guide and Tutorial, CA: Wavefunction, 2017, pp. 435-518.
29. Maldonado F, Stashans A. "DFT modeling of benzoyl peroxide adsorption on α-Cr2O3 (0001) surface," Surface Review and Letters, 2016, 23(5): 1650037.
30. Guo-Liang D, Zhen-Hua L, Jing L, Wen-Ning W, Kang-Nian F. "Deep Oxidation in the Oxidative Dehydrogenation Reaction of Propane over V2O5(001): Periodic DFT Study," The Journal of Physical Chemistry C, 2012, 116 (1): 807-817.
31. Satyajit D, Nand K, Plaban J, Ramesh C. "DFT Insight on Oxygen Adsorbed Pt Trimer Cluster (Pt3) for CO Oxidation," Computational and Theoretical Chemistry, 2017, 1114(1): 1-7.
32. Liu C, Li G., Emiel E, Hensen J, Pidko E. "Relationship between acidity and catalytic reactivity of faujasite zeolite: A periodic DFT study," Journal of Catalysis, 2016, 344(1): 570–577.
33. Liu C, Tranca I, van Santen RA, Hensen RJ, Pidko EA. "Scaling relations for acidity and reactivity of zeolites," The Journal of Physical Chemistry C, 2017, 121(42): 23520-23530.
34. David R. "CRC Handbook of Chemistry and Physics, 84th Edition.," in Section 10, Atomic, Molecular, and Optical Physics; Ionization Potentials of Atoms and Atomic Ions, 84th ed., Boca Raton, Florida: CRC Press., 2003, pp. (10-178)-(10-179).
35. Fukui K., "Role of frontier orbitals in chemical reactions," Science, 1982, 218(4574): 747-754.
36. Lillehaug S., "A Theoretical Study of Cr/oxide Catalysts for Dehydrogenation of Short Alkanes," The University of Bergen, Department of Chemistry, 2006.
37. Lugo HJ, Lunsford JH. "The dehydrogenation of ethane over chromium catalysts," Journal of Catalysis, 1985, 91(1): 155-166.
38. Michorczyk P, Ogonowski J, Kuśtrowski P, Chmielarz L. "Chromium oxide supported on MCM-41 as a highly active and

selective catalyst for dehydrogenation of propane with CO2," Applied Catalysis A: General, 2008, 349(1-2): 62-69.
39. Michorczyk P, Ogonowski J, Zeńczak K. "Activity of chromium oxide deposited on different silica supports in the dehydrogenation of propane with CO2–a comparative study," Journal of Molecular Catalysis A: Chemical, 2011, 349(1-2): 1-12.
40. Bailey BC, Schrock RR, Kundu S, Goldman AS, Huang Z, Brookhart M. "Evaluation of Molybdenum and Tungsten Metathesis Catalysts for Homogeneous Tandem Alkane Metathesis," Organometallics, 2009, 28(1): 355-360.
41. Chen K, Bell AT, Iglesia E., "Kinetics and Mechanism of Oxidative Dehydrogenation of Propane on Vanadium, Molybdenum, and Tungsten Oxides," Journal of Physical Chemistry B, 2000, 104(1): 1292-1299.
42. Jupp A, Johnstone T, Stephan D. "The Global Electrophilicity Index as a Metric for Lewis Acidity," Dalton Transactions, 2018, 45(1): 1-7.
43. Yun Y, Araujo JR, Melaet G, Baek J, Archanjo BS, Oh M, Alivisatos AP, Somorjai GA. "Activation of Tungsten Oxide for Propane Dehydrogenation and Its High Catalytic Activity and Selectivity," Catalysis Letters, 2017, 147(3): 622–632.
44. Salamanca-Guzmán M, Licea-Fonseca YE, Echavarría-Isaza A, Faro A, Palacio-Santos LA. "Oxidative dehydrogenation of propane with cobalt, tungsten and molybdenum based materials," Revista Facultad de Ingeniería Universidad de Antioquia, 2017, 84(1): 97-104.

APPENDIX

Table A1. Molecular Properties of the Catalysts.

Name	*Formula*	*ELUMO (eV)*	*EHOMO (eV)*	*E (eV)*	*E Gap, (eV)*	*CH, η (eV)*	*EN, χ (eV)*	*CP, μ (eV)*	*GEI, ω (eV)*
Chromia	Cr_2O_3	*-2.68*	*-14.51*	*-0.88*	*11.83*	*5.92*	*8.60*	*-8.60*	*3.12*
Mo-Chromia	$CrMoO_3$	*-1.31*	*-14.89*	*-0.73*	*13.58*	*6.79*	*8.10*	*-8.10*	*2.42*
W-Chromia	$CrWO_3$	*0.37*	*-12.80*	*-2.26*	*13.17*	*6.59*	*6.22*	*-6.22*	*1.47*

Table A2. Correlation of Cr-Site Lewis Acidity Results.

	aELUMO (eV)	*aEHOMO (eV)*	*aAc_Cr*	*aCH, η (eV)*	*aEN, χ (eV)*	*aCP, μ (eV)*	*aGEI, ω (eV)*	*pE LUMO (eV)*	*pEHOMO (eV)*	*pAc_Cr*	*pCH, η (eV)*	*pEN, χ (eV)*	*pCP, μ (eV)*	*pGEI, ω (eV)*
aELUMO (eV)	*1.00*													
aEHOMO (eV)	*0.58*	*1.00*												
aAc_Cr	*-1.00*	*-0.57*	*1.00*											
aCH, η (eV)	*0.01*	*-0.81*	*-0.02*	*1.00*										
aEN, χ (eV)	*-0.82*	*-0.94*	*0.81*	*0.57*	*1.00*									
aCP, μ (eV)	*0.82*	*0.94*	*-0.81*	*-0.57*	*-1.00*	*1.00*								
aGEI, ω (eV)	*-0.90*	*-0.87*	*0.90*	*0.42*	*0.99*	*-0.99*	*1.00*							
pELUMO (eV)	*-0.89*	*-0.89*	*0.88*	*0.46*	*0.99*	*-0.99*	*1.00*	*1.00*						
pEHOMO (eV)	*-0.88*	*-0.90*	*0.87*	*0.48*	*0.99*	*-0.99*	*1.00*	*1.00*	*1.00*					
pAc_Cr	*-0.99*	*-0.49*	*1.00*	*-0.12*	*0.75*	*-0.75*	*0.85*	*0.79*	*0.82*	*1.00*				
pCH, η (eV)	*0.85*	*0.92*	*-0.84*	*-0.53*	*-1.00*	*1.00*	*-0.99*	*0.83*	*-1.00*	*-0.78*	*1.00*			
pEN, χ (eV)	*0.88*	*0.90*	*-0.87*	*-0.47*	*-0.99*	*0.99*	*-1.00*	*-1.00*	*-1.00*	*-0.82*	*1.00*	*1.00*		
pCP, μ (eV)	*-0.88*	*-0.90*	*0.87*	*0.47*	*0.99*	*-0.99*	*1.00*	*-1.00*	*1.00*	*0.82*	*-1.00*	*-1.00*	*1.00*	
pGEI, ω (eV)	*0.73*	*0.98*	*-0.72*	*-0.67*	*-0.99*	*0.99*	*-0.95*	*-0.96*	*-0.97*	*-0.65*	*0.98*	*0.97*	*-0.97*	*1.00*

Table A3. Correlation of M-Site Lewis Acidity Results.

	αELUMO (eV)	αEHOMO (eV)	αAc_M	αCH, η (eV)	αEN, χ (eV)	αCP, μ (eV)	αGEI, ω (eV)	pELUMO (eV)	pEHOMO (eV)	pAc_M	pCH, η (eV)	pEN, χ (eV)	pCP, μ (eV)	pGEI, ω (eV)
αELUMO (eV)	1.00													
αEHOMO (eV)	-0.79	1.00												
αAc_Cr	1.00	-0.78	1.00											
αCH, η (eV)	0.81	-1.00	0.80	1.00										
αEN, χ (eV)	0.77	-1.00	0.75	1.00	1.00									
αCP, μ (eV)	-0.77	1.00	-0.75	-1.00	-1.00	1.00								
αGEI, ω (eV)	-0.83	0.32	-0.84	-0.35	-0.28	0.28	1.00							
pELUMO (eV)	-1.00	0.80	-1.00	-0.82	-0.78	0.78	0.82	1.00						
pEHOMO (eV)	-0.83	1.00	-0.82	-1.00	-0.99	0.99	0.38	0.84	1.00					
pAc_Cr	1.00	-0.83	1.00	0.85	0.81	-0.81	-0.79	-1.00	-0.87	1.00				
pCH, η (eV)	0.56	-0.95	0.54	0.94	0.96	-0.96	-0.01	-0.58	-0.93	0.62	1.00			
pEN, χ (eV)	0.92	-0.97	0.90	0.98	0.96	-0.96	-0.54	-0.92	-0.98	0.94	0.85	1.00		
pCP, μ (eV)	-0.92	0.97	-0.90	-0.98	-0.96	0.96	0.54	0.92	0.98	-0.94	-0.85	-1.00	1.00	
pGEI, ω (eV)	0.90	-0.98	0.89	0.98	0.97	-0.97	-0.51	-0.91	-0.99	0.93	0.86	1.00	-1.00	1.00

Table A4. Correlation of O-Site Lewis Acidity Results.

	αELUMO (eV)	αEHOMO (eV)	αAc_O	αCH, η (eV)	αEN, χ (eV)	αCP, μ (eV)	αGEI, ω (eV)	pELUMO (eV)	pEHOMO (eV)	pAc_O	pCH, η (eV)	pEN, χ (eV)	pCP, μ (eV)	pGEI, ω (eV)
αELUMO (eV)	1.00													
αEHOMO (eV)	-0.92	1.00												
αAc_Cr	-0.46	0.77	1.00											
αCH, η (eV)	0.99	-0.97	-0.60	1.00										
αEN, χ (eV)	-0.77	0.47	-0.20	-0.66	1.00									
αCP, μ (eV)	0.77	-0.47	0.20	0.66	-1.00	1.00								
αGEI, ω (eV)	-0.84	0.98	0.87	-0.91	0.30	-0.30	1.00							
pELUMO (eV)	-0.89	1.00	0.82	-0.95	0.39	-0.39	1.00	1.00						
pEHOMO (eV)	-0.79	0.96	0.91	-0.88	0.22	-0.22	1.00	0.98	1.00					
pAc_Cr	0.00	0.39	0.89	-0.16	-0.63	0.63	0.55	0.47	0.62	1.00				
pCH, η (eV)	-1.00	0.90	0.42	-0.98	0.81	-0.81	0.80	0.86	0.75	-0.05	1.00			
pEN, χ (eV)	0.85	-0.99	-0.86	0.92	-0.32	0.32	-1.00	-1.00	-0.99	-0.53	-0.82	1.00		
pCP, μ (eV)	-0.85	0.99	0.86	-0.92	0.32	-0.32	1.00	1.00	0.99	0.53	0.82	-1.00	1.00	
pGEI, ω (eV)	-0.84	0.98	0.87	-0.91	0.30	-0.30	1.00	1.00	1.00	0.55	0.80	-1.00	1.00	1.00

Table A5. Correlation of Lewis Acidity and Catalyst Surfaces' Molecular Descriptors.

	ELUMO (eV)	EHOMO (eV)	CH, η (eV)	EN, χ (eV)	CP, μ (eV)	GEI, ω (eV)	E Gap (eV)	aAc_Cr	aAc_M	aAc_O	pAc_Cr	pAc_M	pAc_O
ELUMO (eV)	1.00												
EHOMO (eV)	0.80	1.00											
CH, η (eV)	0.69	0.13	1.00										
EN, χ (eV)	-0.97	-0.93	-0.48	1.00									
CP, μ (eV)	0.97	0.93	0.48	-1.00	1.00								
GEI, ω (eV)	-1.00	-0.82	-0.67	0.97	-0.97	1.00							
E Gap (eV)	0.69	0.13	1.00	-0.48	0.48	-0.67	1.00						
aAc_Cr	-0.50	-0.91	0.28	0.71	-0.71	0.52	0.29	1.00					
aAc_M	-0.95	-0.95	-0.44	1.00	-1.00	0.96	-0.43	0.74	1.00				
aAc_O	-1.00	-0.77	-0.73	0.95	-0.95	1.00	-0.73	0.45	0.93	1.00			
pAc_Cr	-0.57	-0.95	0.19	0.77	-0.77	0.60	0.19	1.00	0.80	0.53	1.00		
pAc_M	-0.92	-0.97	-0.35	0.99	-0.99	0.93	-0.35	0.80	1.00	0.89	0.85	1.00	
pAc_O	-0.91	-0.98	-0.34	0.99	-0.99	0.92	-0.33	0.81	0.99	0.89	0.86	1.00	1.00
Average of Ac(s)	-0.81	-0.92	-0.23	0.90	-0.90	0.82	-0.23	-	-	-	-	-	-

Table A6. The Geometry of Different Structures Optimized by the PM3 method.

Molecular probe and other small molecules		
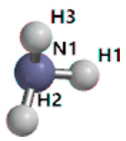 *Ammonia*	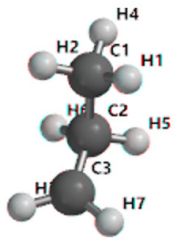 *Propane*	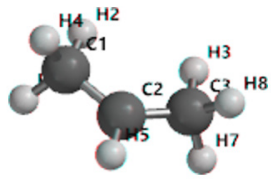 *Propyl-2*
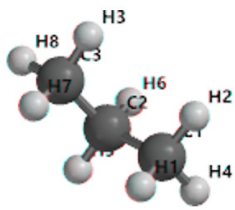 *Propyl-1*	 *Hydrogen atom*	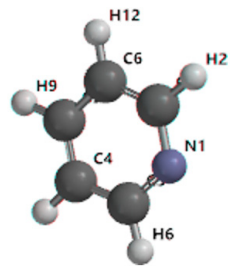 *Pyridine*

Table A6. The Geometry of Different Structures Optimized by the PM3 method (continued).

Catalyst clusters

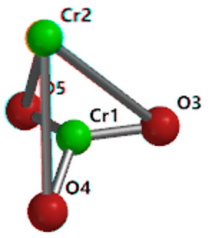

Unmodified cluster

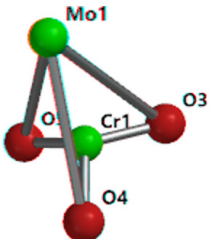

Mo-modified cluster

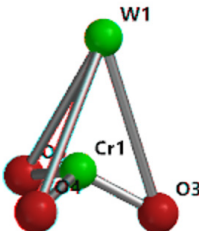

W-modified cluster

Adsorption of ammonia probe on chromium, Cr-sites

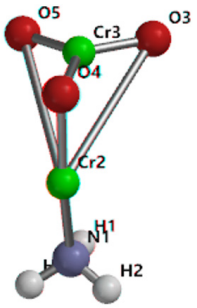

Unmodified cluster

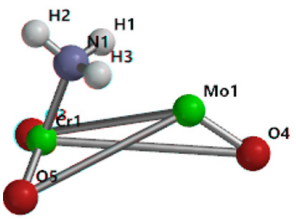

Mo-modified cluster

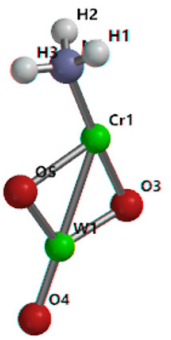

W-modified cluster

Adsorption of ammonia probe on modified M-sites (M = W, Mo)

Unmodified one, M = Cr, remaining unchanged

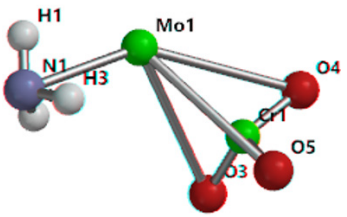

M = Mo-site

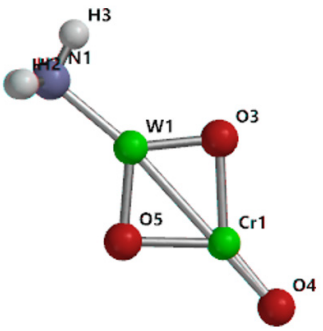

M = W-site

Adsorption of ammonia probe on oxygen, O-sites

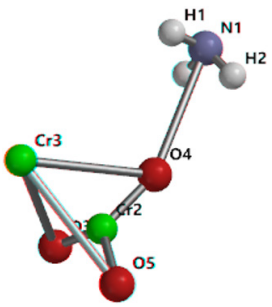

Unmodified cluster

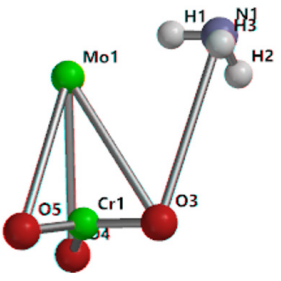

Mo-modified cluster

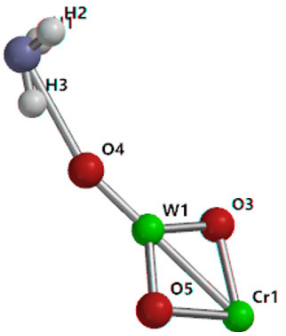

W-modified cluster

Table A6. The Geometry of Different Structures Optimized by the PM3 method (continued).

Adsorption of pyridine probe on chromium, Cr-sites

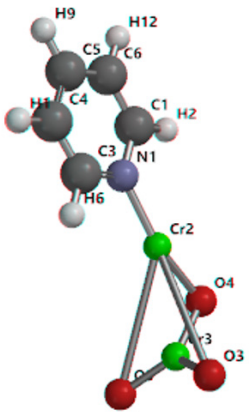

Unmodified cluster

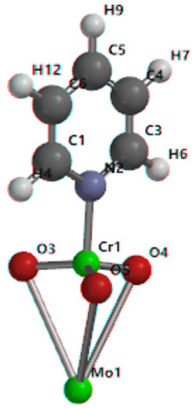

Mo-modified cluster

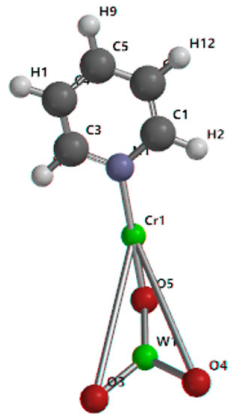

W-modified cluster

Adsorption of pyridine probe on modified M-sites (M = W, Mo)

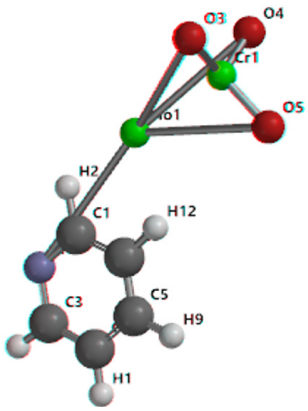

M = Mo-site

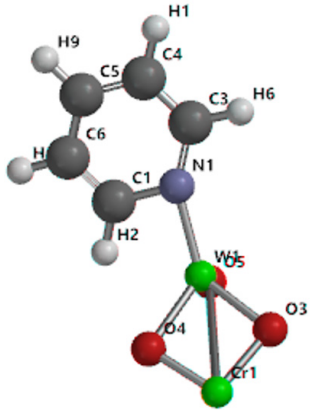

M = W-site

Unmodified one, M=Cr, remaining unchanged

Adsorption of pyridine probe on oxygen, O-sites

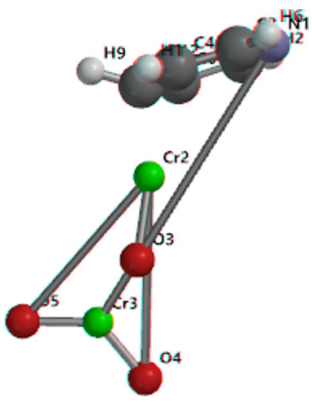

Mo-modified cluster

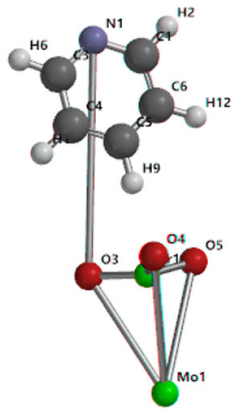

Mo-modified cluster

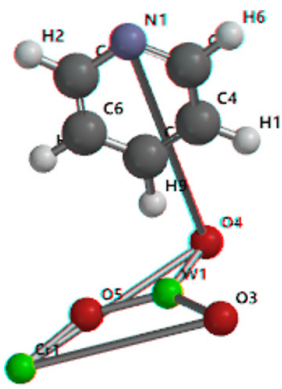

Mo-modified cluster